Title
A SEARCH FOR SPECTRAL FEATURES IN THE SUB-MILLIMETER BACKGROUND RADIATION

Authors
Mather, John C.
Werner, Michael W.
Richards, P.L.

Publication Date
1971-10-01

Submitted to Astrophysical Journal (Letters [illegible])

A SEARCH FOR SPECTRAL FEATURES IN THE SUB-MILLIMETER BACKGROUND RADIATION

John C. Mather, Michael W. Werner, and P. L. Richards

October 1971

AEC Contract No. W-7405-eng-48

Submitted to Astrophysical Journal (Letters Section)

LBL-148
Preprint

UNIVERSITY OF CALIFORNIA

Lawrence Berkeley Laboratory
Berkeley, California

AEC Contract No. W-7405-eng-48

A SEARCH FOR SPECTRAL FEATURES IN THE SUB-MILLIMETER BACKGROUND RADIATION

John C. Mather, Michael W. Werner, and P. L. Richards

October 1971

LBL-148

A Search for Spectral Features in the Sub-Millimeter Background Radiation

John C. Mather†, Michael W. Werner§, and P. L. Richards

Department of Physics, University of California

and

Inorganic Materials Research Division,
Lawrence Berkeley Laboratory,
Berkeley, California 94720

ABSTRACT

We have made mountaintop observations at 1% spectral resolution of atmospheric and sky emission in the ν=6-14 cm^{-1} frequency region. No emission features were found which can be related to the diffuse, isotropic flux F_o=1.3 x 10^{-9} W cm^{-2} Sr^{-1} reported from rocket and balloon experiments. We can thus set a lower limit to the spectral width of any feature responsible for F_o. This limit varies from 0.25 cm^{-1} (for ν=13.5 cm^{-1}) to 0.5 cm^{-1} (for ν<10 cm^{-1}) and is equal to 0.4 cm^{-1} over most of the 10-12 cm^{-1} region. Since we exclude the possibility that the radiation lies in a single narrow line such as might arise from a maser process in the upper atmosphere, our observations seem to require an extraterrestrial origin for F_o.

† Fannie and John Hertz Foundation Fellow

§ Work partially supported by NASA Grants NGL 05-003-272 and NGR 05-003-432

Direct measurements of the diffuse isotropic sub-millimeter background radiation indicate an energy flux considerably in excess of that expected from an extrapolation of the 2.7°K blackbody field implied by measurements at lower frequencies. High altitude rocket experiments (Shivanandan, Houck, and Harwit, 1968; Houck and Harwit, 1969; Pipher, et al., 1971) indicate a total flux $F_o=1.3 \times 10^{-9}$ W cm^{-2} Sr^{-1} over the ν = 7.5-25 cm^{-1} band, but give no information on the spectral distribution within the band. The radiation is observed to be isotropic within at least 10%. F_o represents 25 times more energy than is expected in this spectral region from a 2.7°K blackbody field.

If spread uniformly over the 7.5-25 cm^{-1} band, F_o represents a spectral intensity ($I_\nu = 2.5 \times 10^{-14}$ W cm^{-2} Sr^{-1}/cm^{-1}), which is greater by a factor of 2 to 3 than the upper limits on I_ν at 7.6 cm^{-1} and 17.9 cm^{-1} determined by Thaddeus (1970) from upper limits on the excitation of low-lying states of CN and CH in interstellar space. This apparent discrepancy can be resolved in terms of a peak in the background flux in the 10-12 cm^{-1} region reported by Muehlner and Weiss (1970) from measurements at moderate spectral resolution with a balloon-borne photometer. All of the above results are consistent (Caroff and Petrosian, 1971) with a 2.7°K blackbody field with an additional strong emission feature in the 10-12 cm^{-1} region contributing a flux roughly equal to F_o.

If the radiation represented by the flux F_o is distributed on a galactic (or, especially) on an extragalactic scale, it is the major form of radiant energy density present (≈ 1.7 eV/cm^3) and therefore of great significance. Theoretical attempts to explain this radiation on the basis of a galactic origin (Wagoner, 1969) or an extragalactic origin (Caroff and Petrosian, 1971) meet with severe difficulties.

The experiment reported here was an attempt to detect this background emission with flux F_o in the 10-12 cm^{-1} region by ground based observations at high spectral resolving power. A similar study (Beery et al, 1971) carried out at Mauna Kea found no features unambiguously related to F_o. However, Beery et al report a narrow emission feature at 11.7 cm^{-1} which cannot easily be explained as of atmospheric origin and thus might be related to F_o. In our observation we do not find the 11.7 cm^{-1} feature. The only discrete spectral features definitely seen are those expected from atmospheric O_2 and H_2O. We are thus able to set a lower limit $\delta\nu_L$ as a function of ν to the width of any feature contribution the flux F_o in the (7.5-14 cm^{-1}) spectral region.

II. EXPERIMENTAL PROCEDURES

Our observations were carried out with a high throughput rapid scan Fabry-Perot spectrometer, shown schematically in Figure 1. Radiation from a 6° field of view on the sky was focused by a teflon lens and chopped at 550 Hz against an ambient temperature blackbody. The reflector at the front of the instrument could be rotated around the optic axis to permit spectra to be taken at any zenith angle. It could also be pointed down into a liquid nitrogen cooled blackbody which served as a calibration source and established a temperature scale for our spectra. A 3m long section of 7.5 cm diameter polished brass pipe transmitted the chopped beam to the interior of a laboratory building where the spectrometer (discussed below) was located. The detector was a liquid helium cooled InSb electronic bolometer, fed by a germanium cone (Vystavkin et al, 1970). A cooled transformer matched the detector to a room temperature FET preamp. Following amplification and phase sensitive detection the signal was fed to a signal averaging system which accumulated several hours of data by superposing successive spectral scans.

The spectrometer consisted of low and high finesse 3" diameter Fabry-Perot etalons (FP_1 and FP_2) in a series, with FP_2 operated in first order to act as an order sorter for FP_1. The reflectors in FP_2 were 125 line per inch nickel mesh, giving a finesse $N \approx 8$ at 1 mm; in FP_1, they were 300 lpi mesh having $N \approx 70$ (Ulrich, Renk, and Genzel, 1963). Radiation with $\nu \geq 15\ cm^{-1}$ was rejected by a capacitative grid low pass filter (Ulrich, 1967). In the 10-14 cm^{-1} region, we operated up to the third order of FP_1 and attained resolution $\approx .05\ cm^{-1}$ at 10 cm^{-1}. We also carried out some observations at $\nu < 10\ cm^{-1}$. Here the signal was so small that it was necessary to work in the first order of FP_2 or FP_1 alone, adding a polyethylene grating scatter filter to reject high orders. One of the reflectors of FP_1 was mounted on a microscope stage, which was driven by a stepping motor to scan the spectrum by varying the reflector spacing. When FP_2 was used simultaneously, its spacing was varied in such a way that the two etalons always transmitted the same frequency although they were set for different orders. The rate of scan was 0.1 cm^{-1}/sec and individual sweeps were accumulated for several hours with the signal averaging system. This rapid scanning greatly reduced the influence of slow fluctuations of the atmospheric water vapor emission on the averaged spectra. The noise temperature of our entire system was ≈ 20°K pk-pk for 1 sec of integration and 0.1 cm^{-1} bandwidth.

In order to be above much of the atmospheric water vapor, we carried out our observations at the University of California's Barcroft Laboratory at an altitude of 12,500 ft. on White Mountain in Eastern California between April 27, 1971 and May 3, 1971. During the observing period, the atmospheric water vapor content was between 0.5 and 2 precipitable mm so that windows with greater than 50% transparency were available at frequencies up to 14 cm^{-1} (Nolt et al, 1971).

III. RESULTS

Figure 2 shows a first order spectrum of sky emission in the 7.5 - 13 cm^{-1} region, together with a theoretical atmospheric spectrum. The experimental spectrum in Figure 2 is divided into two sections by a vertical line. These represent the ranges of actual experimental scans. The data in each range were obtained under different conditions, of water vapor, resolution, and noise. Each section of the experimental curve is the weighted average of several individual runs. The individual spectra consisted of 1 to 3 hours of observation of the sky divided by a calibration spectrum of the liquid N_2 blackbody to establish a temperature scale. Because we measure the temperature difference ΔT between the sky and an ambient temperature blackbody, emission features (corresponding to a hotter sky and smaller ΔT) protrude downward on the plots. The theoretical spectra were prepared by using the compilation of H_2O lines given by Burch (1968) and the O_2 lines listed by Gebbie et al (1969) to calculate atmospheric emission for an assumed atmospheric temperature $T_o = 270°K$, pressure $p = 0.67$ atm, and various quantities of H_2O. The emission was convolved with our instrumental function to obtain the theoretical spectra shown. The theoretical curve shown corresponds to 1.25 precipitable mm of H_2O for $\nu > 10.6$ cm^{-1} and 1.5 precipitable mm for $\nu < 10.6$ cm^{-1}. The theoretical and experimental spectra show the expected strong lines of H_2O at 10. 7 and 12.68 cm^{-1} . The continuum emission is due to the wings of the higher frequency H_2O lines. The close agreement between the theoretical spectrum and our experimental data is a useful check on our calibration procedure. Since the atmospheric H_2O above White Mountain is concentrated in a thin layer of (presumably) uniform temperature (O'Connor et al, 1968), the atmospheric transmission $t(\nu)$ may be estimated from our spectra as $t(\nu) = \Delta T(\nu)/T_o$. On the basis of this model the ordinate in Figures 2-4 varies from zero to 100 percent transmission. Note that $t(\nu) \approx 70\%$ in the 11.5 cm^{-1} window, rising to > 90% for $\nu < 10$ cm^{-1}.

Figure 3 is a third order spectrum of the 10-14 cm^{-1} region at three times higher resolving power than in Figure 2. Note the O_2 lines at 12.3 and 14.2 cm^{-1}. The intent of this observation was to search with high resolution and low noise for sharp spectral features. To attain this goal, some sacrifice was made in the completeness of rejection of unwanted orders from the interferometer. Such contamination is largely responsible for the reduction in transmission in the low frequency side as compared with theory or the data of Figure 2.

We find no evidence for any features on our experimental spectra which can definitely be related to F_o. If we assume that $F_o = 1.3 \times 10^{-9}$ W cm^{-2} Sr^{-1} is concentrated in a line of width $\delta\nu$ at frequency ν, this line will appear on our spectra as a feature of depth

$$T(\nu,\Delta\nu) = \frac{F_o t(\nu)}{2kc\nu^2\Delta\nu} = \frac{1570t(\nu)}{\nu^2\Delta\nu}\ {}^\circ K \qquad (1)$$

Here, k = Boltzmann's constant, c is the speed of light, and $\Delta\nu$ is the full width at half height of the line as it actually appears on the spectrum. If the feature is sharp, then $\Delta\nu$ equals the experimental resolution $\Delta\nu_I$. In this case $T(\nu,\Delta\nu_I)$ is very large (a 100°K line for $\Delta\nu_I = 0.08$ cm^{-1} at $\nu = 11.7$ cm^{-1}). No sharp feature approaching this strength appears in any of our spectra. If the feature is much broader than $\Delta\nu_I$, its actual width $\delta\nu$ is observed and the depth is accordingly reduced. Our sensitivity to narrow features is greatest in third order (Figure 3), while our sensitivity to broad features is greatest in first order (Figure 2). Very broad features cannot be detected because the atmospheric emission spectrum is not known accurately. By comparing the theoretical and epxerimental spectral shapes we can set a lower limit $\delta\nu_L(\nu)$ to the width as a function of frequency of any spectral features contributing the flux F_o. On this basis, we arrive at the values for $\delta\nu_L(\nu)$ tabulated below. The corresponding upper limits on the temperature of the feature calculated from Equation 1 lie in the range 20-30°K.

The arrows in Figures 2 and 3 at 11.7cm^{-1} indicate the frequency at which Beery et al (1971) reported detection of an emission feature with T = 30° and $\Delta\nu$ = 0.2 cm^{-1}. In data obtained at various times throughout the day and night and at several zenith angles, we find no evidence for an emission feature at this frequency greater than the peak-to-peak noise, which is typically ≈ 5°K. The weak feature appearing at 12 cm^{-1} in Figure 3 does recur in several individual spectra and may be real.

Figure 4 shows a low resolution spectrum of sky emission in the 6-9 cm^{-1} region. The main feature observed is the 6.11 cm^{-1} H_2O line. We see no evidence for the diffuse emission reported in the 7-9 cm^{-1} region by several groups observing under conditions similar to ours (Harries and Burroughs, 1970; Gebbie et al, 1971) and attributed to the water vapor dimer $(H_2O)_2$. If the theoretically predicted dimer opacity (Viktorova and Zhevakin, 1967) is extrapolated to the atmospheric conditions for high altitude observations, the expected emission is somewhat less than the noise level in Figure 4.

IV. SUMMARY AND CONCLUSIONS

A consistent interpretation of all data on the sub-millimeter background requires that the flux F_o is concentrated in the 10-12 cm^{-1} region. Our observations rule out the existence of a single narrow line in this region carrying this much flux, such as might arise from an atmospheric maser. Thus, there seems to be no plausible terrestrial origin for this flux. Additionally, all features definitely present in our spectra over the wider region from 6 to 14 cm^{-1} can be attributed to atmospheric O_2 and H_2O. However, our data may be reconciled with the earlier observations in several ways:

A) F_o is present in the 10-12 cm^{-1} region but the width of the feature is $\gtrsim 0.4$ cm^{-1}, corresponding to a line depth $\lesssim 20°K$. Under these circumstances, the line becomes difficult to detect because its width is comparable with the scale of the structure in the atmospheric emission.

B) The radiation is present as a narrow line hidden behind the 12.68 cm^{-1} H_2O line. If the line is actually the 12.68 cm^{-1} H_2O line (say from an interstellar maser) one has the problem that this H_2O transition has an excitation energy of 200 cm^{-1} so that F_o may represent only a small portion of the energy emitted.

C) The radiation is due to a series of lines each contributing a fraction of F_o, clustered in the 10-12 cm^{-1} region. Since any line having width $\Delta\nu_I$ and $T \gtrsim 10°K$ would be apparent on our spectra, at least five such narrow lines would be required.

ACKNOWLEDGMENTS

We wish to thank Dr. C. H. Townes for stimulating our interest in this research and for continued helpful discussions. We are grateful to Drs. J. R. Houck and J. L. Pipher of Cornell University for detector material, to Dr. J. E. Gaustad for the loan of his averaging system, to Dr. D. Cudaback for logistical consultations, and to Mr. W. Brown for programming help. The work at White Mountain was greatly facilitated by outstanding logistical support from Dr. Nello Pace, Messers. M. Antoniou, D. Buser, S. Keachie, and other members of the White Mountain Research Station staff.

This work was performed under the auspices of the U. S. Atomic Energy Commission.

REFERENCES

1. Beery, J. G., Martin, T. Z., Nolt, I. G., and Wood, C. W. 1971, Nature Physical Science 230, 36.
2. Burch, D. E. 1968, J. Opt. Soc. Am. 58, 1383.
3. Caroff, L. J. and Petrosian, V. 1971, Nature 231, 378.
4. Gebbie, H. A., Bohlander, G. W., and Pardue, G. W. F. 1971, Nature 230, 521.
5. Gebbie, H. A., Burroughs, W. J., and Bird, G. R. 1969, Proc. Roy. Soc. London A310, 579.
6. Harries, J. E. and Burroughs, W. J. 1970, Infrared Physics 10, 165.
7. Houck, J. R. and Harwit, M. O. 1969, Ap. J. 157, L45.
8. Muehlner, D. and Weiss, R. 1970, Phys. Rev. Letters 24, 742.
9. Nolt, I., Martin, T. Z., Wood, C. W., and Sinton, W. M. 1971, J. Atm. Sci. 28, 238.
10. O'Connor, J. T., Welch, W. J., and Tayeb, A. M. 1968, Berkeley Space Science Laboratory Internal Report.
11. Pipher, J. L., Houck, J. R., Jones, B. W., and Marwit, M. O. 1971, Nature 231, 375.
12. Shivanandan, K., Houck, J. R., and Harwit, M. O. 1968, Phys. Rev. Letters 21, 1460.
13. Thaddeus, P. 1970, Results reported at Texas Symposium, Austin. See also Bortolot, V. J., Jr., Clauser, J. F., and Thaddeus, P. 1969, Phys. Rev. Letters 22, 307.
14. Ulrich, R. 1967, Infrared Physics 7, 37.
15. Ulrich, R., Renk, K. R., and Genzel, L. 1963, IEEE Trans. on Microwave Theory and Techniques, M.I.T. 11, 363.

REFERENCES (cont.)

16. Viktorova, A. A., and Zhevakin, S. A. 1967, Sov. Physics-Doklady 11, 1065.

17. Vystavkin, A. N., Gobenkov, A. N., Listvin, V. N., and Migulin, V. V. 1970, Brooklyn Polytechnic Conference on Millimeter Waves.

18. Wagoner, R. V. 1969, Nature 224, 481.

TABLE I

Limits on Width of Sub-Millimeter Emission Feature

Contributing Flux $F_o = 1.3 \times 10^{-9}$ W/cm^2 Sr

Freq. Range	Total Observing Time	$\delta\nu_L(\nu)$
13.15-13.9 cm^{-1}	22 min.	0.25 cm^{-1}
11.1-12.1	7 (Fig. 2), 288 (Fig. 3)	0.4
10.65-11.1	120	0.1
7.5-10.65	200	0.5

$\delta\nu_L$ = minimum width of supposed feature. Limits are average values for each frequency range and vary from one frequency range to another because of differences in atmospheric transmission and observing conditions.

FIGURE CAPTIONS

Figure 1: Sub-millimeter Fabry-Perot Spectrometer, described in detail in the text. FP_1 and FP_2 are high and low finesse Fabry-Perot etalons.

Figure 2: Observed 7.5-13 cm^{-1} sky emission spectrum (solid) compared with theoretical spectrum (dashed) for 1.25 precipitable mm H_2O ($\nu > 10.6$ cm^{-1}) and 1.5 precipitable mm ($\nu < 10.6$ cm^{-1}). ΔT, the temperature difference between the sky and an ambient temperature blackbody, is plotted vs. frequency. Emission features protrude downwards on this plot. The principal features are lines of atmospheric H_2O (10.87, 12.68 cm^{-1}) and O_2 (14.2 cm^{-1}). The vertical line separates section of the sky spectrum made under different observing conditions. Arrow at 11.7 cm^{-1} shows position of emission feature reported by Beery et al (1971). No sharp features which can be related to F_o appear on the spectrum.

Figure 3: 10-14 cm^{-1} sky emission spectrum observed in third order (solid), compared with theoretical spectrum (dashed) for 1 precipitable mm H_2O. Note the O_2 lines at 12.3 and 14.2 cm^{-1}. This spectrum contains a substantial contribution from unwanted orders from the interferometer and so underestimates the transmission in the windows. The arrow at 11.7 cm^{-1} shows the position of the emission feature reported by Beery et al (1971). No sharp features which can be related to F_o appear on the spectrum.

FIGURE CAPTIONS (cont.)

Figure 4: Sky emission in the 6-9 cm^{-1} region (solid) obtained at lower resolution than Figure 2, compared with a theoretical spectrum for 1 precipitable mm H_2O (dashed). Total observation time = 40 minutes. The main feature appearing is the 6.11 cm^{-1} H_2O line. Note the absence of any strong features in the 7-9 cm^{-1} region which could be attributed to the water vapor dimer, $(H_2O)_2$.

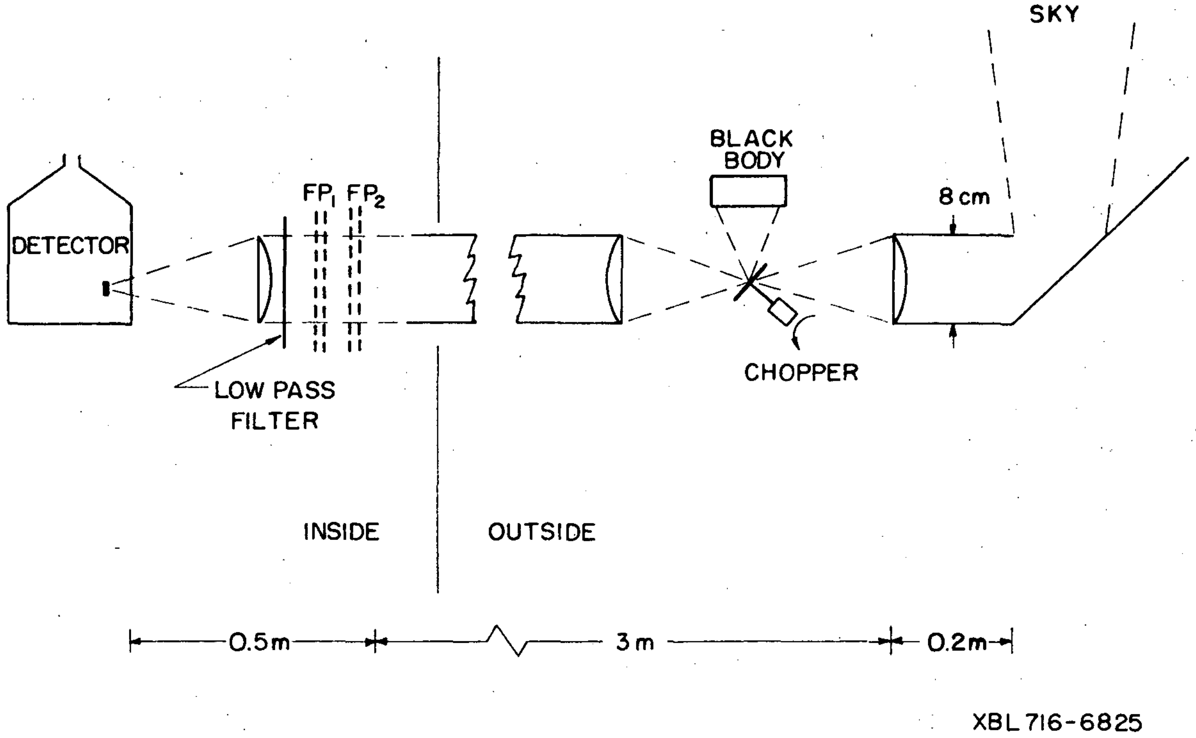
SKY
BLACK BODY
8 cm
FP1 FP2
DETECTOR
CHOPPER
LOW PASS FILTER
INSIDE
OUTSIDE
0.5m
3 m
0.2m
XBL 716-6825

Fig. 1

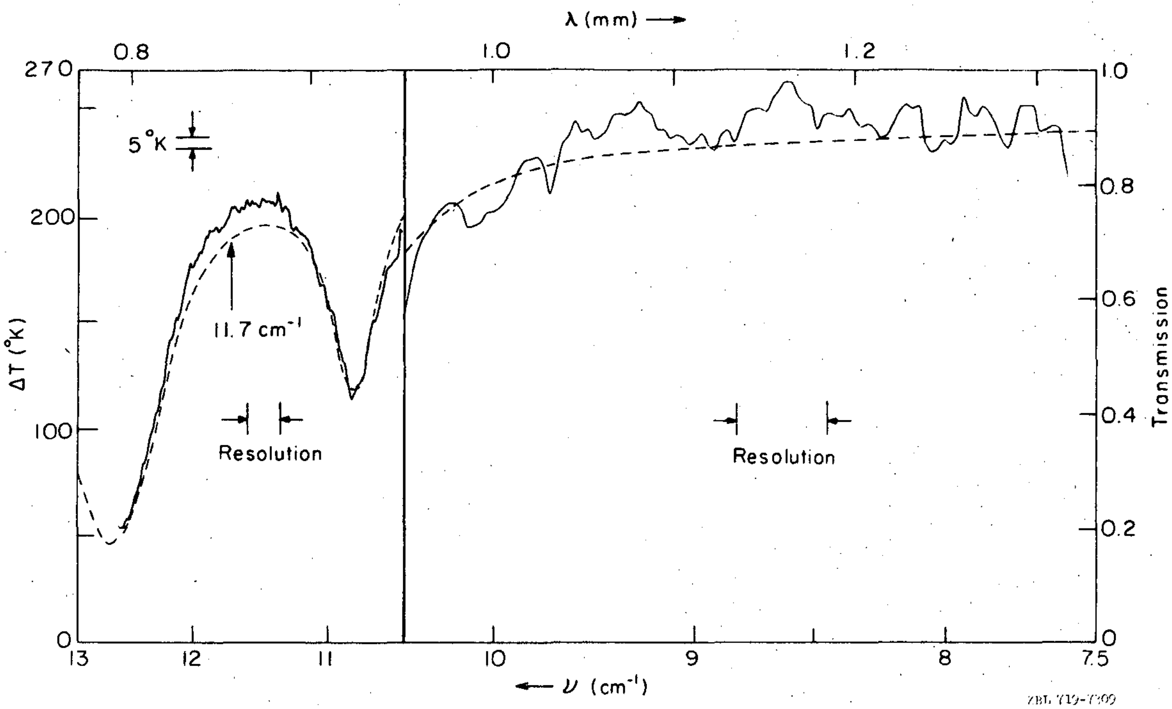
λ (mm) ⟶
0.8
1.0
1.2
270
200
100
0
5 °K
11.7 cm⁻¹
Resolution
Resolution
ΔT (°K)
1.0
0.8
0.6
0.4
0.2
0
Transmission
13
12
11
10
9
8
7.5
⟵ ν (cm⁻¹)

Fig. 2

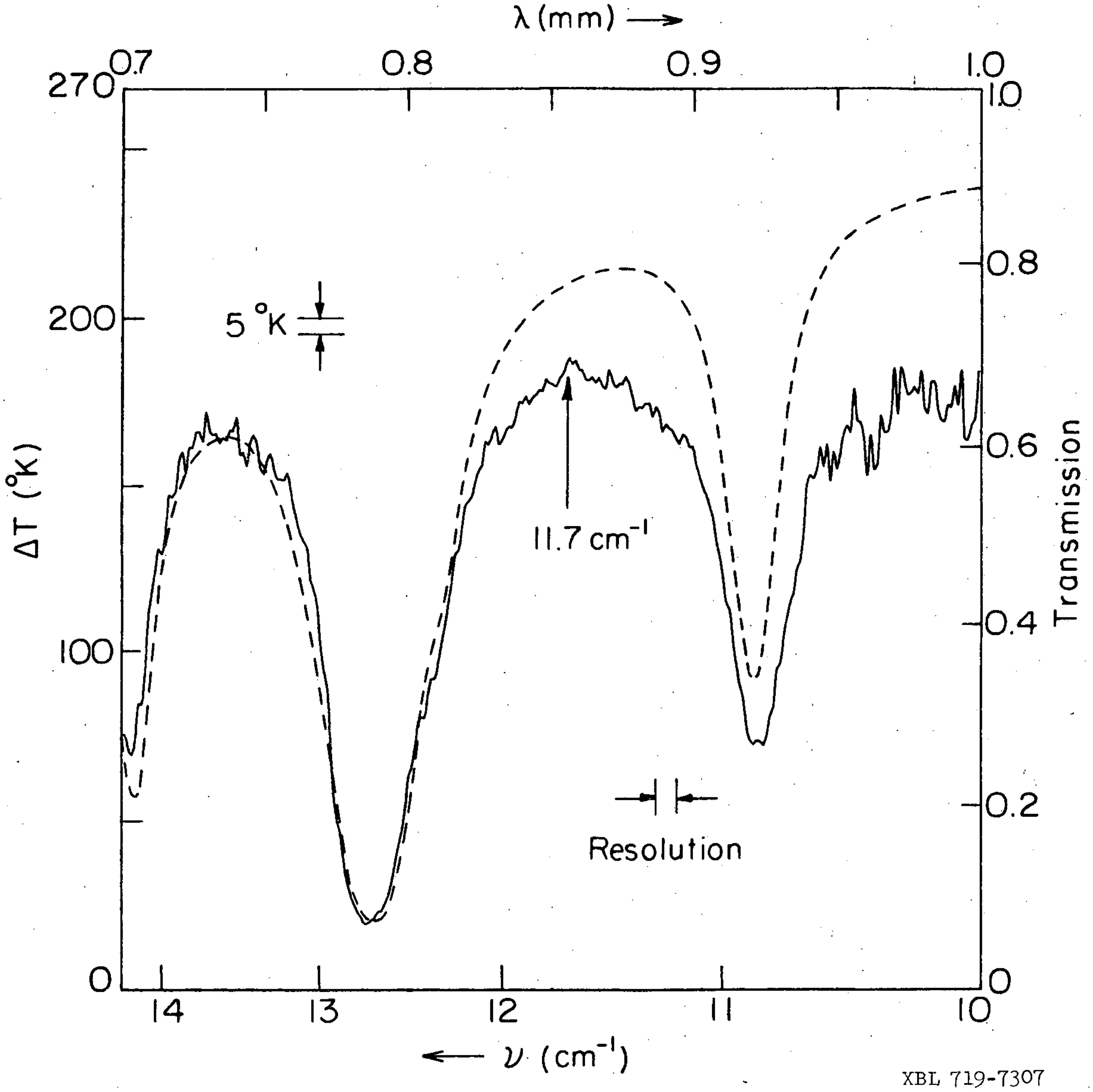

XBL 719-7307

Fig. 3

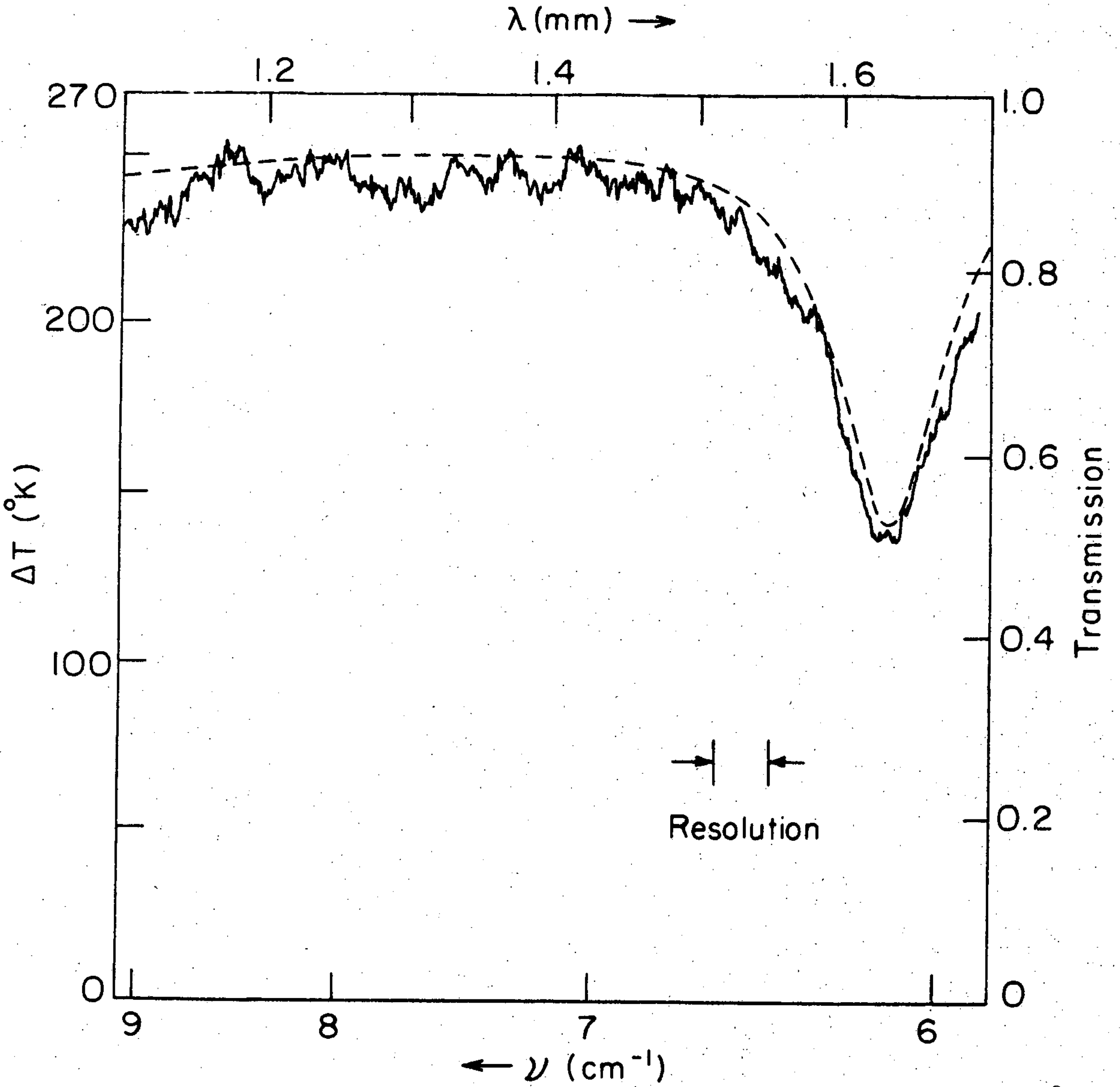

XBL 719-7308

Fig. 4

TECHNICAL INFORMATION DIVISION
LAWRENCE BERKELEY LABORATORY
UNIVERSITY OF CALIFORNIA
BERKELEY, CALIFORNIA 94720